Dependence of the Transitional Properties of Polystyrene-Based Side-Chain Liquid-Crystalline Polymers on the Chemical Nature of the Mesogenic Group

C. T. Imrie,[†] T. Schleeh, and F. E. Karasz*

Department of Polymer Science and Engineering, University of Massachusetts, Amherst, Massachusetts 01003

G. S. Attard

Department of Chemistry, University of Southampton, Southampton SO9 5NH, England

ABSTRACT: The synthesis and characterization of side-chain liquid crystal polymers based on atactic polystyrene and derivatized with differing mesogenic groups are described. These groups are cyano-, methoxy-, nitro-, and fluoroazobenzene and cyanobiphenyl. In each case a butyl spacer is used to link the mesogenic group to the backbone. The cyano- and nitro-substituted azobenzenes exhibit a partially interdigitated smectic A phase, whereas the methoxy- and fluoro-substituted azobenzenes exhibit a smectic A phase in which the side chains overlap to a considerably greater extent. The dependence of the clearing temperatures on the molecular structure of the mesogenic unit was found to be in accord with the behavior observed for low molar mass mesogens and other side-chain polymers having differing backbones. In contrast, the dependence of the glass transition temperature on the chemical nature of the mesogenic moiety appears to be influenced by the structure of the backbone.

Introduction

Side-chain liquid crystal polymers have attracted interest since their discovery over 12 years ago.[1] Over this period, research has centered not only on the application potential of this novel class of materials but also on fundamental aspects, in particular on the competition between configurational entropy and liquid-crystalline order. In the initial investigations the majority of side-chain polymers reported were based on either poly-(siloxane)s[2] or poly(methacrylate)s and poly(acrylate)s.[3] In more recent years a wide range of backbones has been used for synthesizing side-chain liquid crystal polymers including, for example, poly(vinyl ether)s,[4] poly(phosphazene)s,[5,6] and poly(tartrate)s.[7] Several of these systems, notably poly(siloxane)s and poly(phosphazene)s, have particularly low glass transition temperatures as a result of the inherent flexibility of the polymer backbone. But most of the proposed applications for these materials, such as information storage or nonlinear optics, in fact require a high glass transition temperature. Thus, as part of a systematic program to develop new materials for advanced electro-optic technologies, we have undertaken a systematic investigation of the properties of side-chain liquid crystal polymers derived from polystyrene. The choice of polystyrene was based on the assumption that a more rigid backbone would endow the final polymers with higher glass transition temperatures, and indeed we have shown this to be the case.[8] In this contribution we consider the effect of varying the chemical constitution of the mesogenic moiety on the thermal properties of the polymer and on the ultrastructure of the mesophase. The structures of the polymers as well as the acronyms we use to describe them are listed in Table I.

Experimental Section

The polymers were prepared through reactions shown in Scheme I. The coupling of a diazotized 4-substituted aniline
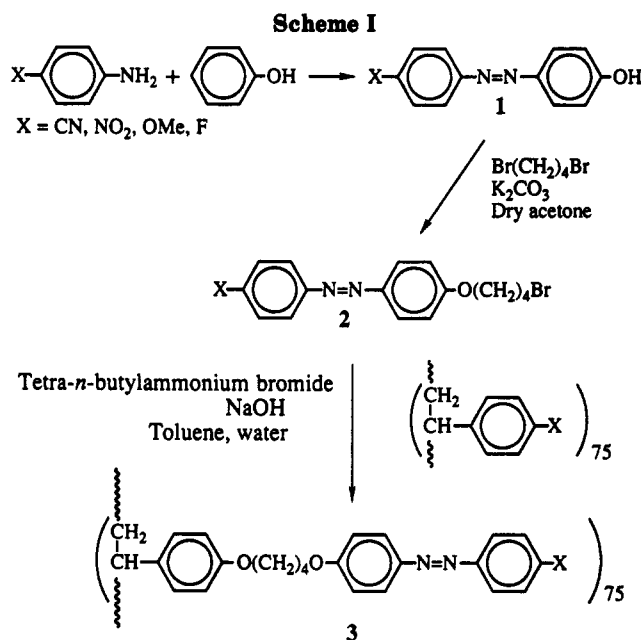
with phenol to yield 4-hydroxy-4'-substituted azobenzene, **1**, was performed by a standard method.[9] 4-Cyano-4'-hydroxybiphenyl was used as received from American Tokyo Kasei, Inc. All other materials were used as received from Aldrich Chemical Co.

Scheme I

Table I
Structures of the Polymers and Their Acronyms
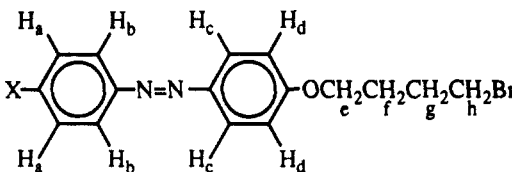
Z	X	acronym	Z	X	acronym
N=N	CN	Azo-CN	N=N	F	Azo-F
N=N	NO₂	Azo-NO₂		CN	Bip-CN
N=N	OMe	Azo-OMe			

* To whom correspondence should be addressed.
† Present address: Department of Chemistry, University of Aberdeen, Meston Walk, Old Aberdeen AB9 2UE, Scotland.

Table II
Elemental Analyses and Spectroscopic Data for the Monomers

X	elem anal.[a]	δ/ppm	ν/cm⁻¹
CN	C, 57.02 (56.99)	2.05 (m, 4 H, H_f, H_g), 3.50)	2227 (CN
	H, 4.60 (4.50)	(t, 2 H, H_h), 4.10 (t, 2 H,	stretch)
	N, 11.51 (11.73)	H_e), 7.02 (m, 2 H, H_d),	
		7.85 (m, 6 H, H_a, H_b, H_c)	
NO₂	C, 50.86 (50.81)	2.05 (m, 4 H, H_f, H_g), 3.50	1344 (NO
	H, 4.24 (4.26)	(t, 2 H, H_h), 4.10 (t, 2 H,	stretch)
	N, 11.10 (11.11)	H_e), 7.03 (m, 2 H, H_d),	
		7.95 (m, 4 H, H_b, H_c),	
		8.35 (m, 2 H, H_a)	

[a] Parentheses denote theoretical values.

Monomers 2. The reaction of a substituted phenol with a 10-fold excess of an α,ω-dibromoalkane has been described in detail elsewhere.[10] The synthesis and characterization of the 4-methoxyazobenzene-,[11] 4-fluoroazobenzene-,[12] and 4-cyanobiphenyl[13]-substituted bromoalkanes are given elsewhere. The 4-cyanoazobenzene- and 4-nitroazobenzene-substituted compounds were prepared in an analogous fashion and recrystallized twice with hot filtration from ethanol. The elemental analyses and spectroscopic data for the monomers are listed in Table II. The monomers are mesogenic, and their properties will be the subject of a separate paper.[8]

Polymers 3. The phase-catalyzed reaction of a bromo-substituted monomer, **2**, with poly(4-hydroxystyrene) (average molecular weight = 9000–11 000; Polysciences, Inc.) was performed by the method described by Crivello et al.[10] We have extended the reaction time, however, from 24 h up to 72 h to ensure essentially complete derivatization of the backbone. Infrared spectroscopy is a particularly useful tool with which to monitor the extent of backbone substitution, because the very strong OH stretch absorption present in the spectrum of the parent polymer is not evident in that of the final polymer.[12] The yields of the derivatized polymers are typically in the region of 65%, and we have not observed any appreciable molecular weight degradation during the derivatization process. Only the elemental analyses for the new polymers are listed in Table III, but Table IV gives the spectroscopic characteristics of these materials and, for comparison, those of the polymer reported previously.

Characterization. The proposed structures of the polymers and their intermediates were verified by IR spectroscopy using an IBM System 9000 FTIR spectrometer and by ¹H-NMR spectroscopy using a Varian XL200 NMR spectrometer. These were further confirmed by elemental analysis performed by the University of Massachusetts Microanalytical Laboratory.

Thermal Characterization. The thermal properties of the polymers were investigated by differential scanning calorimetry using a Perkin-Elmer DSC-7 differential scanning calorimeter calibrated using an indium standard. Two samples of each polymer were run, and the average values of the enthalpies are quoted in Table V. Peak maxima are used to indicate the transition temperatures. The heating rate in all instances was 10 °C min⁻¹, and the resultant traces are qualitatively identical to those previously published for analogous materials.[11,13] The textures of the liquid-crystal phases exhibited by the polymers were studied by polarizing microscopy using a Carl-Zeiss polarizing microscope equipped with a Linkam hot stage. The ultrastructure of the mesophases was probed by X-ray diffraction using Cu Kα₁ radiation. These studies were performed with annealed powder samples. The sample preparation involved heating the polymer to a temperature approximately 50 °C above its clearing point, cooling at 2 °C min⁻¹ to a temperature approximately 10 °C above the clearing temperature, equilibrating at that temperature for several minutes, and then cooling at 0.2 °C min⁻¹ into the clearing range. The polymer was held

at that temperature for approximately 10 min and subsequently cooled to room temperature at 0.2 °C min⁻¹. In addition, from Azo-NO₂ it was possible to obtain fibers that were drawn from the liquid-crystalline melt. The small-angle (SAXS) and wide-angle (WAXS) X-ray scattering patterns were recorded on flat film with sample-to-film distances of 253 and 78.5 mm, respectively.

Results and Discussion

The thermal properties of the polymers are listed in Table V. Qualitatively, the DSC traces of the polymers were identical, each showing a second-order transition corresponding to the glass transition and a first-order transition corresponding to the clearing transition. To obtain an optical texture for use in assigning a phase, each polymer was heated to approximately 10 °C above its clearing point and allowed to cool at 0.2 °C min⁻¹ through the phase transition. Bâtonnets developed at the transition and coalesced to yield a focal-conic fan texture indicative of a layered structure. In addition, regions of homeotropic texture formed, a result implying that the director of the phase is orthogonal to the layer planes. Consequently, the observed phase was assigned as smectic A, an assignment that was supported by the X-ray diffraction experiments to be described later.

The thermal properties of Azo-CN have been reported by Crivello et al.,[10] and, although the transition temperatures show good agreement[14] (allowing for a small molecular weight effect[15]), the phase assignment is very different. Crivello et al. describe the optical texture for this polymer as consisting of very small domains that remain essentially unchanged even after annealing for several days. We found this to be the case also for other polystyrene-based liquid crystal polymers and so developed the technique of cooling the polymer slowly through the transition rather than simply annealing.[16] Using this method, we obtained a very well-defined focal-conic fan texture for Azo-CN, a result that unambiguously indicates a smectic arrangement. On the basis of their X-ray results, however, Crivello et al. assigned this phase as a nematic, because they obtained no reflections in the small-angle region. As we have already noted, however, in order to obtain good X-ray diffraction patterns for these polymers the powders have to be annealed and even then the exposure times are very long. Crivello et al. also cite a low enthalpy change, which is in reasonable agreement with that reported here and is normally indicative of a nematic–isotropic transition. It is surprising that the smectic A–isotropic transition is accompanied by such a small entropy change; we will discuss this later.

The glass transition temperatures of the polymers are in the order Azo-OMe ≈ Azo-CN > Azo-NO₂ ≈ Azo-F ≈ Bip-CN. It should be noted that the spread of the glass transition temperatures is approximately 14 °C, a value indicating that the structure of the mesogenic group not only is important in determining the liquid-crystal properties of the polymer but also has an effect, although significantly smaller, on the glass transition. The efficiency of the terminal group in stabilizing a liquid-crystal phase is Azo-CN > Azo-NO₂ > Azo-OMe > Azo-F > Bip-CN, and this is in complete accord with the behavior of low molar mass mesogens.[17] The entropies of transition fall into two groups; Azo-F and Azo-OMe exhibit significantly higher entropies than Azo-CN and Azo-NO₂. The entropy of transition exhibited by Bip-CN is particularly low for a smectic–isotropic transition, but this is presumably a consequence of the close proximity of the glass transition. The entropies of transition suggest that the Azo-F and Azo-OMe polymers form one modification of the smectic

Table III
Elemental Analyses for the Polymers

polymer	formula	mol wt	C calc	C found	H calc	H found	N calc	N found
Azo-CN	$(C_{25}H_{23}N_3O_2)_n$	$(397.5)_n$	75.54	75.03	5.83	5.69	10.57	10.76
Azo-NO$_2$	$(C_{24}H_{23}N_3O_4)_n$	$(417.4)_n$	69.05	69.08	5.55	5.57	10.07	10.23
Azo-F	$(C_{24}H_{23}FN_2O_2)_n$	$(390.4)_n$	73.82	73.34	5.94	6.06	7.18	7.30
Bip-CN	$(C_{25}H_{23}NO_2)_n$	$(369.4)_n$	81.27	81.23	6.27	6.25	3.79	3.84

Table IV
Spectroscopic Data for the Polymers

Z	X	δ/ppm	ν/cm^{-1}	λ_{max}/nm
N=N	CN	1.95 (m, 7 H, H$_f$, H$_g$, H$_a$, H$_b$), 4.00 (m, 4 H, H$_e$, H$_h$), 6.65, 6.90 (m, 6 H, H$_c$, H$_d$, H$_i$), 7.85 (m, 6 H, H$_j$, H$_k$, H$_l$)	2227 (CN stretch)	361
N=N	NO$_2$	2.01 (m, 7 H, H$_f$, H$_g$, H$_a$, H$_b$), 4.05 (m, 4 H, H$_e$, H$_h$), 6.70, 6.95 (m, 6 H, H$_c$, H$_d$, H$_i$), 7.85 (m, 4 H, H$_j$, H$_k$) 8.25 (m, 2 H, H$_l$)	1344 (NO stretch)	375
N=N	OMe	1.92 (m, 7 H, H$_f$, H$_g$, H$_a$, H$_b$), 3.85, 3.98 (m, 7 H, H$_e$, H$_h$, OCH$_3$), 6.65, 6.90 (m, 8 H, H$_c$, H$_d$, H$_i$, H$_l$), 7.80 (m, 4 H, H$_j$, H$_k$)		357
N=N	F	1.93 (m, 7 H, H$_f$, H$_g$, H$_a$, H$_b$), 3.99 (m, 4 H, H$_e$, H$_h$), 6.63, 6.94, 7.05 (m, 8 H, H$_c$, H$_d$, H$_i$, H$_l$), 7.80 (m, 4 H, H$_j$, H$_k$)		347
	CN	1.45, 1.95 (m, 7 H, H$_f$, H$_g$, H$_a$, H$_b$), 4.00 (m, 4 H, H$_e$, H$_h$), 6.62, 6.90 (m, 6 H, H$_c$, H$_d$, H$_i$), 7.42, 7.55, 7.62 (m, 6 H, H$_j$, H$_k$, H$_l$)	2225 (CN stretch)	294

Table V
Thermal Properties of the Polymers

polymer	T_g/°C	T_{Cl}/°C	ΔH/(J g^{-1})	$\Delta S/R$
Azo-CN	86	161	3.94	0.43
Azo-NO$_2$	78	152	4.14	0.49
Azo-OMe	89	144	11.8	1.37
Azo-F	76	129	10.7	1.25
Bip-CN	75	105	1.00	0.12

Figure 1. SAXS pattern obtained from the fibers drawn from the liquid-crystalline melt of Azo-NO$_2$ and slowly cooled. The orientation direction is orthogonal with respect to the reflections.

Figure 2. WAXS pattern for a powder sample of Azo-F.

A phase whereas the remaining polymers exhibit a different variant on the smectic A structure. This possibility was investigated using X-ray diffraction and indeed found to be the case.

The X-ray diffraction patterns obtained from the fibers drawn from the liquid-crystalline melt of Azo-NO$_2$ confirm the assignment of the phase as a smectic A. In the SAXS pattern (Figure 1), a single sharp reflection was evident on the equator, a result indicating that the director of the smectic phase is oriented perpendicular to the fiber axis and that this is an orthogonal phase. In the WAXS pattern, two sharp reflections were seen on the equator at low angles, and these were assigned as the first- and second-order reflections arising from the smectic layers. The remaining polymers were studied as annealed samples as a result of great difficulties encountered in trying to produce suitable fibers. These patterns exhibited a sharp ring at low angles, a pattern resulting from the smectic layers, and a diffuse halo at wide angles. In addition, the WAXS patterns for
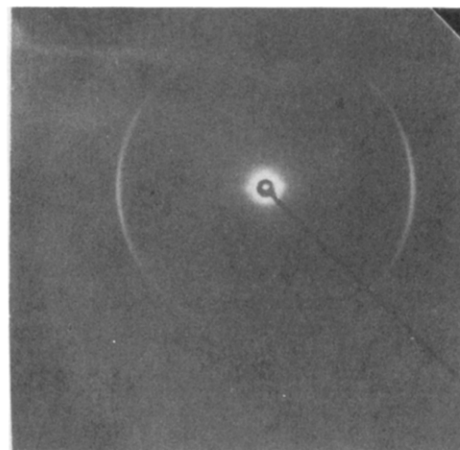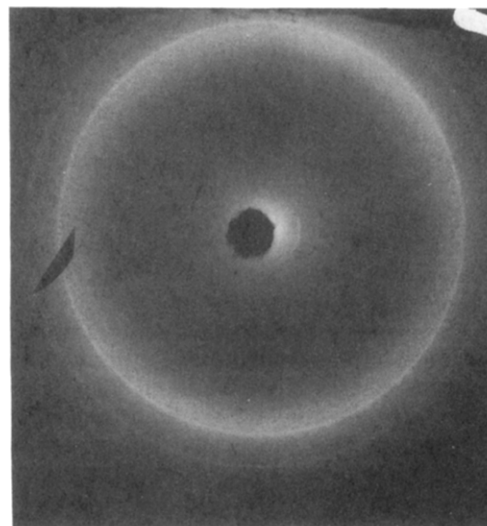
Azo-F showed a sharp reflection at $2\theta = 22.26°$ (see Figure 2); this reflection has been observed for another polystyrene-based liquid crystal copolymer,[18] although its origin is somewhat unclear. Figures 2 and 3 reveal also that over a period of several days Azo-F and Azo-OMe tended to partially crystallize. The X-ray pattern for Bip-CN had only the diffuse halo at wide angles; this pattern may be the result of the high viscosity of the isotropic melt close to the clearing temperature. The observation of the smectic A phase by microscopy and calorimetry may be the result of surface forces.

Table VI lists the values of 2θ for the first-order reflection observed and the associated layer spacing d for each polymer. In addition, Table VI gives the estimated all-trans molecular length l of the side chains, both including and excluding the segment of the backbone attached to the side chain, and lists the d/l ratios. When we include the backbone in our calculations, we see that Azo-NO$_2$
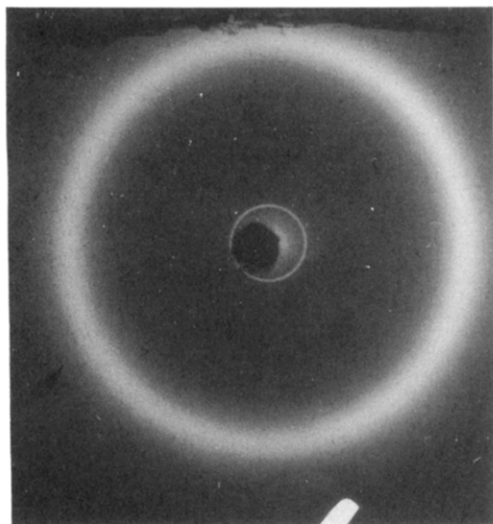
Figure 3. WAXS pattern for a powder sample of Azo-OMe.

Table VI
X-ray Data for the Polymers

polymer	$2\theta/\deg$	$d/\text{Å}$	$l_A{}^a/\text{Å}$	d/l_A	$l_B{}^b/\text{Å}$	d/l_B
Azo-NO$_2$	2.52	29.2	26.2	1.11	17.6	1.66
Azo-OMe	4.91	23.2	27.3	0.85	18.7	1.24
Azo-CN	2.83	31.2	26.3	1.19	18.0	1.73
Azo-F	4.46	19.8	25.2	0.79	16.7	1.19

^{a} l_A is the estimated all-trans molecular length of the side chain including the styrene moiety. ^{b} l_B is the molecular length excluding the styrene group.

and Azo-CN exhibit d/l ratios of approximately 1.15, whereas for Azo-OMe and Azo-F this ratio is just 0.8. When we exclude the backbone, these ratios increase to approximately 1.7 and 1.2, respectively. These differences suggest, as was implied by the entropies of transition, that Azo-NO$_2$ and Azo-CN have a smectic phase that differs in structure from the smectic phase of Azo-OMe and Azo-F.

To understand the differences in the structure of smectic A phases, it is helpful to consider the different structures of the smectic A phases of polymers and of low molar mass compounds. For low molar mass liquid crystals, it is a straightforward task to deduce the structure of the smectic A phase solely from a knowledge of the layer spacing. For side-chain polymers, however, the task is less straightforward, because the role of the backbone in the formation of the smectic phase is unclear. There are at least six possible types of smectic A phases exhibited by side-chain liquid crystal polymers (Figure 4). These six structures are conveniently split into two sets of three, which differ according to the backbone arrangement. In one set of structures, panels a, c, and e in Figure 4, the backbone is confined by the smectic field and lies between the layers. This arrangement has been described in terms of a microphase separation.[19] In the second set of structures, panels b, d, and f in Figure 4, the conformation of the backbone is largely unaffected by the smectic field and possesses essentially a three-dimensional isotropic structure. Each set shows three structural variations of the smectic phase. In the first of these, termed S$_{A_1}$, the side chains overlap fully and the d/l ratio approaches unity. If the backbone is indeed sandwiched between the layers, then the dimensions of the polymer must be included in l in order to obtain such a ratio; for the isotropic backbone, however, only the side chain needs to be considered. The other extreme is the S$_{A_2}$ phase, in which the side chains exhibit no interdigitation and thus d/l is 2. Between these
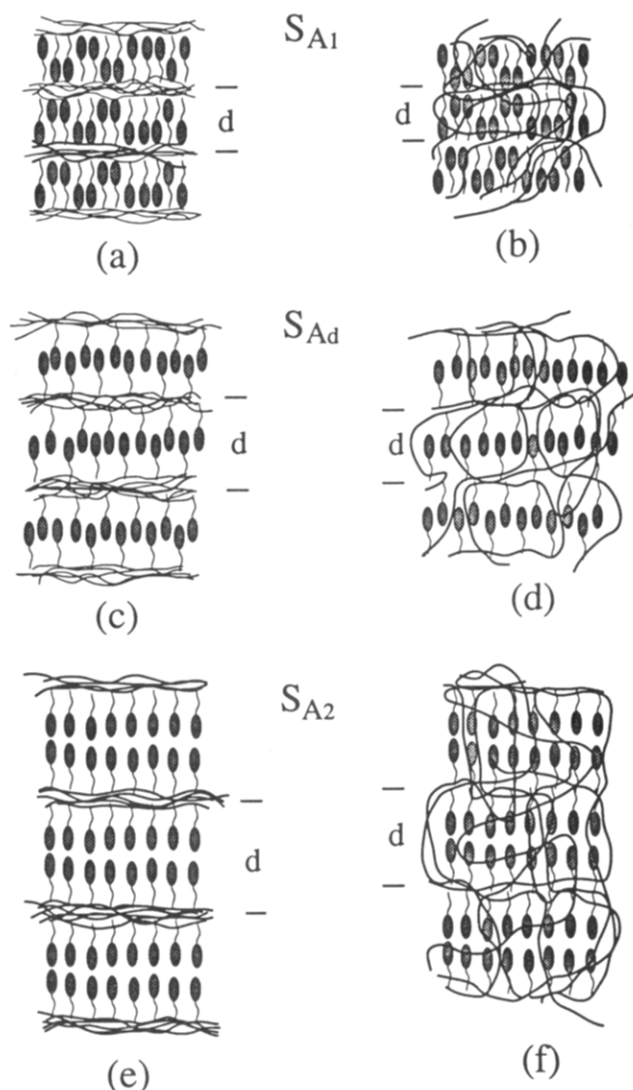

Figure 4. Smectic A phases exhibited by side-chain polymers.

extrema are a range of partially interdigitated phases, termed S$_{A_d}$, in which $1 < d < 2l$.

A first inspection of the data presented in Table VI suggests that the backbone is in an isotropic arrangement for two reasons. First, phase structures of materials having cyano and nitro groups are known to be dominated by the formation of antiparallel pairs, which serve to minimize the dipolar energy. Figure 5 shows two possible local structures that might be deduced from the X-ray data. For Figure 5a, backbone interactions are neglected, and the local structure with minimized dipolar energy results. By contrast, it is difficult to conceive of a driving force that might be responsible for the structure shown in Figure 5b. The second piece of evidence suggesting an isotropic arrangement of the backbone is the d/l ratio exhibited by Azo-OMe and Azo-F; for both compounds the ratio is less than unity if we include the backbone in our measurements. Figure 6 shows a *possible* local arrangement of the side chains for Azo-OMe, assuming an isotropic backbone. It is important to note that, irrespective of the backbone arrangement assigned to Azo-F, the fluoroazobenzene moieties do not arrange themselves in antiparallel pairs, and this may have very important consequences for the application of these materials.

By referring to the structures shown in Figures 5 and 6, we can readily explain the difference in the entropies of transition. For Azo-OMe and Azo-F, there is considerable overlap between the mesogenic core and the flexible
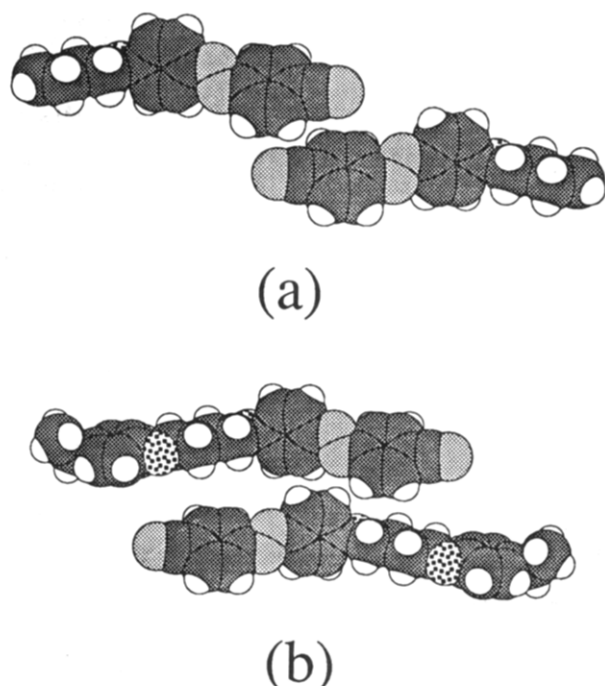
(a)

(b)

Figure 5. Local arrangement of the side chains in the smectic A phase of Azo-CN, allowing for (a) an isotropic arrangement and (b) a confined arrangement of the backbone. Note that, in Figures 5–7, heavily shaded areas denote carbon atoms, lightly shaded areas denote the azo linkages, unshaded areas are hydrogen atoms, and the speckled areas denote oxygen atoms.
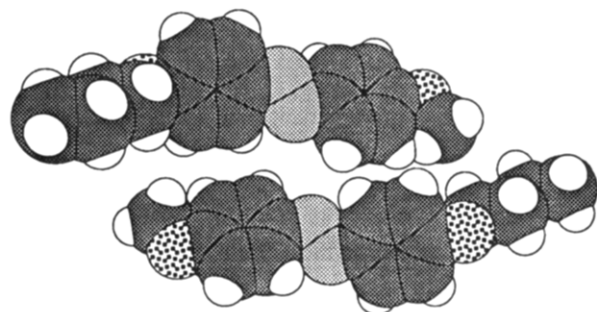

Figure 6. Local arrangement of the side chains in the smectic A phase exhibited by Azo-OMe, allowing for an isotropic arrangement of the backbone.

spacers. This interaction is entropically unfavorable and serves to order the spacer. Therefore, at the clearing transition, there will be a greater contribution to the entropy of transition arising from the conformation change of the spacers for Azo-OMe and Azo-F than for those of Azo-NO$_2$ and Azo-CN. Indeed it is this interaction that drives the microphase separation in low molar mass liquid crystals that is responsible for the formation of smectic phases.[20] It would appear, therefore, that on the basis of these X-ray data the backbone is not confined between the layers by the smectic field.

However, solid-state CP/MAS ^{13}C NMR spectroscopy has revealed that for octyl spacers the spacer actually possesses a number of defects; this is evident in spectra collected using the interrupted decoupling technique.[18] If we assume that the polymer backbone is in fact sandwiched between the layers, then in striving to increase its entropy it can compress the smectic layer and cause the spacer to yield gauche defects. Within this framework, structures such as that shown in Figure 7 are possible; these structures satisfy the X-ray data and allow an antiparallel association of the nitro- and cyano-containing groups. To remove this ambiguity in structure type, it will be necessary to use
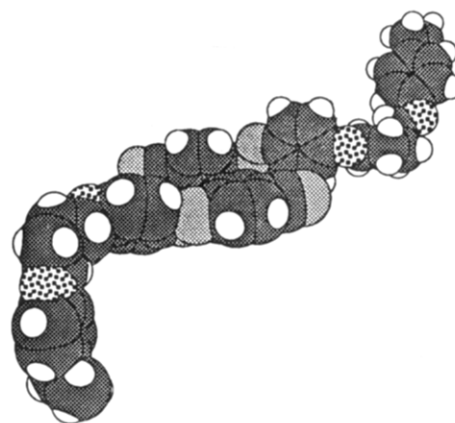

Figure 7. Arrangement of the side chains in the smectic A phase of Azo-CN in which the backbone is confined by the smectic field and the spacer contains gauche defects.

Table VII
Thermal Properties of Side-Chain Liquid-Crystal Polymers Based on Poly(siloxane) Containing Butyl Spacers[23]

Z	X	T_g/°C	T_{Cl}/°C	$\Delta S_{Cl}/R$
COO	OMe	15	95^a	0.28
COO	CN	15	139^b	0.27
OOC	OMe	7	104^a	0.18
OOC	NO$_2$	20	165^b	0.28
OOC	CN	40	174^b	0.48

^{a} Nematic–isotropic transition. ^{b} Smectic A–isotropic transition.

the relative intensities of the Bragg reflections to construct the electron density profiles of the layers.[21]

The poly(acrylate)- and poly(methacrylate)-based analogues of Azo-OMe have been reported,[22] and a comparison of their glass transition temperatures reveals that poly(methacrylate) (T_g = 95 °C) ≈ polystyrene (T_g = 89 °C) > poly(acrylate) (T_g = 75 °C). Their clearing temperatures, however, are in the order poly(acrylate) (T_{NI} = 149 °C) ≈ polystyrene (T_{SI} = 144 °C) ≈ poly-(methacrylate) (T_{NI} = 143 °C).

These differences in transition temperatures are small but are in accord with the general observation that increasing backbone flexibility for a given spacer length and mesogenic group tends to decrease the glass transition temperatures while increasing the clearing point.[8]

It is of interest to compare our results with those from a similar study using poly(siloxane) as the backbone and ester-linked mesogenic units by Richard et al.[23] Table VII summarizes their results, and it is clear that the trends in the clearing temperatures are the same, namely, that the efficiency of the terminal group in promoting liquid crystallinity is CN > NO$_2$ > OMe. The difference in clearing temperature between the nitro- and cyano-substituted polymers is also the same, whereas the clearing temperature for the methoxy-substituted polymer is significantly lower than may have been anticipated on the basis of our results. For Z = COO, the T_{NI} of the methoxy-substituted polymer is 44 °C lower than the cyano-substituted material, and for Z = OOC, this difference increases to 70 °C. By contrast, for the polystyrene-based polymers, this difference is just 17 °C. This may reflect the fact that the transition temperatures of Azo-CN and Azo-NO$_2$ are lower than anticipated, and a possible rationalization for this result invokes the thermal acti-

vation of the cis–trans isomerization of the azo-linkage of these materials. At elevated temperatures, therefore, there is a greater concentration of the cis isomer, which obviously reduces the shape anisometry of the mesogenic unit and hence reduces the clearing temperature. A similar explanation was used to rationalize the anomalously low clearing temperatures of other azo-linked mesogens.[24] The trend in the glass transition temperatures listed in Table VII is CN > NO$_2$ > OMe, and this is not in accord with our findings. The molecular significance of this result is unclear, although presumably it involves interaction between the mesogenic unit and the backbone such that these trends cannot be generalized for all backbones.

Conclusions

We have shown that for polystyrene-based side-chain liquid crystal polymers the effect of varying the structure of the mesogenic group on the clearing temperature is similar to that observed in low molar mass mesogens as well as other side-chain polymers. This is apparently not the case for the glass transition temperatures for which trends appear to be backbone dependent.

References and Notes

(1) See, for example: *Side Chain Liquid Crystal Polymers*; McArdle, C. B., Ed.; Blackie and Sons: Glasgow, U.K., 1989.

(2) Gray, G. W. In *Side Chain Liquid Crystal Polymers*; McArdle, C. B., Ed.; Blackie and Sons: Glasgow, U.K., 1989; Chapter 4.

(3) Percec, V.; Pugh, C. In *Side Chain Liquid Crystal Polymers*; McArdle, C. B., Ed.; Blackie and Sons: Glasgow, U.K., 1989; Chapter 3.

(4) Percec, V.; Lee, M. *Macromolecules* 1991, *24*, 4963.

(5) Allcock, H. R.; Kim, C. *Macromolecules* 1989, *22*, 2596.

(6) Singler, R. E.; Willingham, R. A.; Noel, C.; Friedrich, C.; Bosio, L.; Atkins, E. *Macromolecules* 1991, *24*, 510.

(7) Ujiie, S.; Iimura, K. *Chem. Lett.* 1990, 1031.

(8) Imrie, C. T.; Karasz, F. E.; Attard, G. S. To be submitted for publication.

(9) *Vogel's Textbook of Practical Organic Chemistry*, 4th ed.; Furnias, B. S., Hannaford, A. J., Rogers, V., Smith, P. W. G., Tatchell, A. R., Revisors: Longman Scientific and Technical: New York, 1987.

(10) Crivello, J. V.; Deptolla, M.; Ringsdorf, H. *Liq. Cryst.* 1988, *3*, 235.

(11) Imrie, C. T.; Karasz, F. E.; Attard, G. S. *Macromolecules* 1992, *25*, 1278.

(12) Attard, G. S.; Dave, J. S.; Wallington, A.; Imrie, C. T.; Karasz, F. E. *Makromol. Chem.* 1991, *192*, 1495.

(13) Imrie, C. T.; Karasz, F. E.; Attard, G. S. *Chem. Mater.* 1992, *4*, 1246.

(14) There is an apparent inconsistency in ref 10 between the tabulated value for the clearing point of Azo-CN, 177 °C, and that which can be read from the DSC trace shown by the authors, 168 °C. The glass transition temperature listed in the table agrees well with the DSC trace.

(15) Imrie, C. T.; Karasz, F. E.; Attard, G. S. In preparation.

(16) Imrie, C. T.; Karasz, F. E.; Attard, G. S. *Liq. Cryst.* 1991, *9*, 47.

(17) Gray, G. W. In *The Molecular Physics of Liquid Crystals*; Luckhurst, G. R., Gray, G. W., Eds.; Academic Press: New York, 1979; Chapter 1.

(18) Schleeh, T.; Imrie, C. T.; Rice, D. M.; Karasz, F. E.; Attard, G. S. *J. Polym. Sci., A*, in press.

(19) Tsukruk, V. V.; Shilov, V. V. *Polymer* 1990, *31*, 1793.

(20) Date, R. W.; Imrie, C. T.; Luckhurst, G. R.; Seddon, J. M. *Liq. Cryst.* 1992, *12*, 203.

(21) Davidson, P.; Levelut, A. M. *Liq. Cryst.* 1992, *11*, 469.

(22) Möller, A.; Czajka, U.; Bergmann, V.; Lindau, J.; Arnold, M.; Kuschel, F. *Z. Chem.* 1987, *27*, 218.

(23) Richard, H.; Mauzac, M.; Tinh, N. H.; Sigaud, G.; Achard, M. F.; Hardouin, F.; Gasparoux, H. *Mol. Cryst. Liq. Cryst.* 1988, *155*, 141.

(24) Attard, G. S.; Garnett, S.; Hickman, C. G.; Imrie, C. T.; Taylor, L. *Liq. Cryst.* 1990, *7*, 495.